Jpn. J. Appl. Phys. Vol. 42 (2003) pp. 1470–1474
Part 1, No. 3, March 2003

Quantum Efficiencies of Mg Photocathode under Illumination with 3rd and 4th Harmonics Nd:$LiYF_4$ Laser Light in RF Gun

Terunobu NAKAJYO, Jinfeng YANG, Fumio SAKAI and Yasushi AOKI

R&D Center, Sumitomo Heavy Industries, Ltd. (SHI), Yatocho, Nishitokyo, Tokyo 188-8585, Japan

(Received September 6, 2002; accepted for publication October 30, 2002)

A Mg photocathode for use in a radio-frequency gun was manufactured by a technique of hot isostatic pressing with diamond polishing and tested under a peak electric field of 57 MV/m. A laser cleaning process for the Mg cathode was developed. The quantum efficiency (*QE*) of the Mg cathode before and after the laser cleaning was measured under illumination with 262 nm and 349 nm laser light. A high *QE* of up to 1.0×10^{-3} was achieved under the 262 nm laser-light illumination. The *QE* of the Mg cathode under the 349 nm laser-light illumination was measured to be 2.2×10^{-5}. The dependence of the *QE* on the electric field was measured and compared with a theoretical analysis including the Schottky effect.
[DOI: 10.1143/JJAP.42.1470]

KEYWORDS: mg photocathode, rf gun, high-brightness electron source, quantum efficiency, picosecond laser

1. Introduction

The use of photocathode radio-frequency (rf) guns as high-brightness short-pulse electron sources has been studied for a wide range of applications, such as free-electron lasers,[1] linear colliders,[2] and laser-Compton scattering.[3–5] A typical 1.6-cell S-band (2856 MHz) photocathode rf electron gun with a copper (Cu) photocathode was developed for low-emittance picosecond electron generation by a collaboration between the Brookhaven National Laboratory (BNL), the High Energy Accelerator Research Organization (KEK) and Sumitomo Heavy Industries, Ltd. (SHI).[6–8] A picosecond electron beam with a normalized transverse emittance of $<3\,\pi$mm·mrad at a bunch charge of 1 nC was obtained with the rf gun. The measured quantum efficiency (*QE*) of the copper cathode was as high as 1×10^{-4}.[8,9] However, the development of high-*QE* photocathodes is required for the generation of high-current electron beams, such as multibunch electron generation. Recently, an ultrashort single-bunch electron beam with a high charge was investigated for use in the dynamic studies of ultrafast phenomena by means of pulse radiolysis.[10,11]

Several materials, such as CsI, Cs_2Te, and GaAs, have been studied for use in high-*QE* photocathodes.[12] Quantum efficiencies of up to 10% have been measured in both DC and rf gun arrangements. However, they require ultrahigh vacuum ($<10^{-8}$ Pa) and elaborate cathode preparation systems. The lifetime of these photocathodes is insufficient when they are operating with a high peak electric field (>100 MV/m) on the surface of the cathode. However, these problems could be overcome by the use of a bulk magnesium (Mg) cathode. The Mg cathode, which was tested under an rf field, exhibits 0.2% *QE* under ultraviolet (UV) laser light,[13,14] has a long lifetime and is easy to install in the rf gun. It can also be exposed to ambient air. The work function of Mg is 3.66 eV, which is about 1 eV lower than the Cu work function of 4.65 eV, resulting in a higher quantum efficiency than a Cu cathode for the same drive wavelength of laser light in the rf gun, as in the case of illumination by the 4th harmonic of a Nd:$Y_3Al_5O_{12}$ (Nd:YAG) laser or a Nd:$LiYF_4$ (Nd:YLF) laser.

In order to use Mg in practical applications, we manufactured bulk Mg on a Cu plate by a hot isostatic pressing (HIP) technique. The Mg cathode was installed into a 1.6-cell S-band rf gun driven by an all-solid-state picosecond Nd:YLF laser. The quantum efficiency of the Mg photocathode was measured under illumination with the 3rd and 4th harmonics of a Nd:YLF laser. The effect of laser cleaning was investigated.

2. Experimental Setup

2.1 Mg photocathode

The HIP technique was used to manufacture the Mg photocathode. First, a bulk Mg disk with a diameter of 12 mm and a thickness of 9 mm was press-fitted onto the center of a Cu plate. The purity of Mg was 99.9%. In the press-fitting process, a gap is formed between the Mg and the Cu due to the difference in the thermal expansion coefficients of Mg and Cu, resulting in an electrical discharge and rf breakdown under operation with a high electric field. In order to solve this problem, we connected the Mg disk to the Cu through a diffusion process between Mg and Cu at 673 K and 147 MPa in the next step of the HIP treatment. According to the solidification diagram of Cu–Mg alloy, the eutectic point of Cu–Mg alloy occurs at 758 K, and the temperature used in the HIP treatment was set to be below that temperature. After the HIP treatment, the cathode surface near the boundary between the Mg and the Cu was observed using an optical microscope. Figure 1 shows micrographs of the Mg cathode at magnifications of 200 and 500 times. They indicate that a compound layer was generated between the Mg and the Cu, and that the Mg was tightly connected with the Cu. A vacuum leakage rate of $<10^{10}$ Pa m^3/s was obtained in a helium leak test.

Finally, the Mg surface was polished using diamond-polishing compounds with three different diamond grain sizes of 9 μm, 6 μm and 1 μm. After the polishing, the cathode surface was cleaned by ultrasonic treatment in a hexane solution. Figure 2 shows a photograph of the finished Mg cathode. The size of the cathode was 150 mm in diameter and 20 mm in thickness. The cathode was installed in the half-cell side of an rf gun (described below).

2.2 1.6-Cell s-band RF gun

A schematic diagram of the Mg cathode performance test system is shown in Fig. 3. A 1.6-cell S-band rf gun, constructed under the BNL/KEK/SHI collaboration, was used in the experiment. The rf gun was composed of two

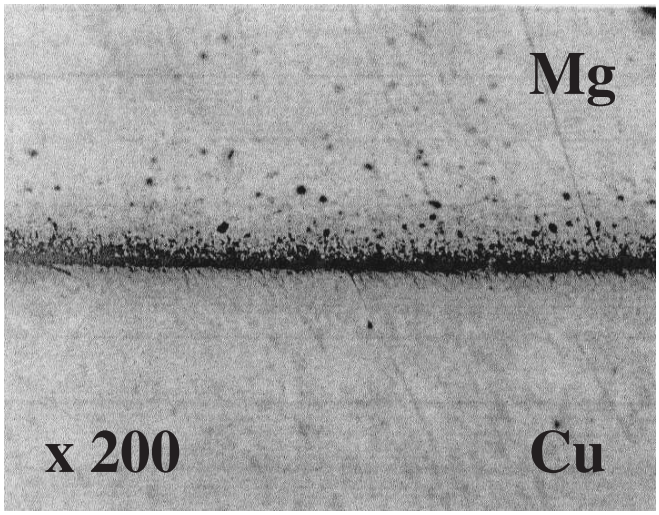

(a)

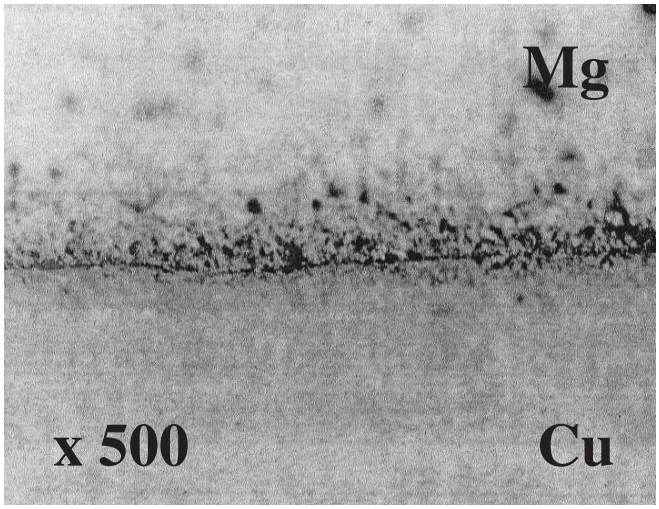

(b)

Fig. 1. Magnesium cathode surface near the boundary of the Mg and the Cu. (a) Magnification of 200 times. (b) Magnification of 500 times.

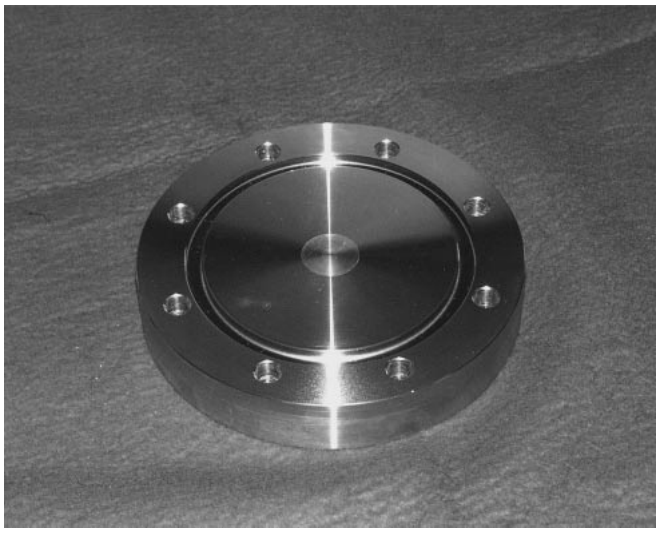

Fig. 2. Mg cathode manufactured by the HIP technique.

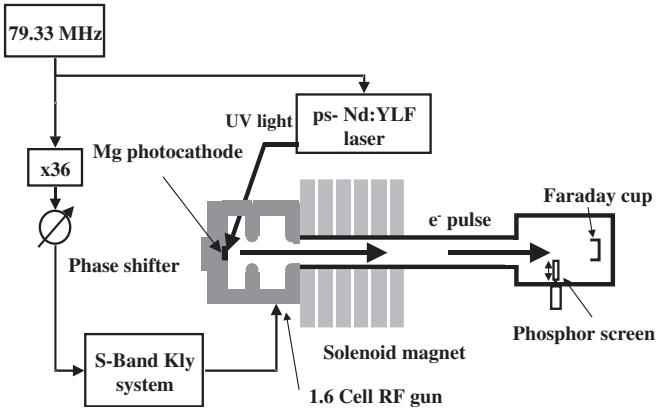

Fig. 3. Schematic diagram of the Mg cathode performance test system.

cells: a half-cell and a full cell. The Mg cathode was located on the side containing the half-cell. The length of the half-cell was designed to be 0.6 times the length of the full cell to reduce beam divergence. Coupling between the waveguide and the cavity was located in the full cell. Coupling between the cells was accomplished via the iris of the cavity. A single solenoid magnet was mounted at the exit of the rf gun to compensate the space-charge emittance. The peak rf input power of the rf gun was 4 MW, which was produced with an s-band klystron. The peak on-axis electric field in the rf gun was 57 MV/m. The repetition rate of the operation was 10 Hz in the experiments.

The electron charge emitted from the Mg photocathode was measured using a Faraday cup (FC) charge monitor, which was located downstream of the rf gun. The current signal from the FC was directly integrated via an electron pulse duration on the digital oscilloscope and converted to electron charge. A phosphor screen, which was installed at the exit of the rf gun, was used to monitor the beam profile. The accelerated energy of the electrons at the exit of the rf gun was 3.0 MeV, which was measured using the phosphor screen and a dipole magnet mounted inside the solenoid magnet.

2.3 Nd:YLF picosecond laser

The rf gun was driven by an all-solid-state laser diode (LD) pumped Nd:YLF picosecond laser. The laser consisted of a passive mode-locked oscillator, a regenerative amplifier and a frequency converter. The oscillator operated at a frequency of 79.33 MHz, the 36th subharmonic of the 2856 MHz accelerating rf. The oscillator output was phase-locked with a reference 79.33 MHz rf signal by dynamically adjusting the cavity length of the oscillator with a semiconductor saturable absorber mirror (SESAM) and a timing stabilizer. The time jitter between the oscillator output and the reference 79.33 MHz rf signal was measured to within a root-mean-square (rms) value of 0.5 ps using a phase detector technique.

A Pockels cell was used to capture a single oscillator laser pulse to amplify the pulse energy up to about 2 mJ in the regenerative amplifier. The repetition rate of the amplifier was 10 Hz in the experiment. The amplified pulse was frequency-converted, by a pair of frequency-conversion nonlinear crystals, to 349 and 262 nm UV light, with maximum pulse energies of 0.5 and 0.2 mJ, respectively.

The UV pulse energy was varied by a polarizer and a half-wavelength plate. The pulse duration of the UV laser had a 10 ps full-width at half maximum (FWHM). The UV light was injected onto the cathode surface at an incident angle of 68° along the electron beam direction.

3. Experimental Results and Discussion

3.1 Laser cleaning

Laser cleaning is an important process that is used in the manufacture of Mg cathodes to improve their effective quantum efficiency. Before laser cleaning of the Mg cathode took place, vacuum baking and rf conditioning of the rf gun were carefully carried out to remove the H_2O absorbed on the surface of the cathode and in the rf cavity. The vacuum pressure was monitored during vacuum baking and rf conditioning was tracked using an ionization gauge at the gun exit. The vacuum pressure after rf conditioning was measured to be 6.0×10^{-7} Pa when the rf was off and 3.0×10^{-6} Pa when the rf was on.

The cleaning laser light utilized the same photocathode-driven 262 nm UV light as the Nd:YLF laser that was used in the experiment. The surface of the Mg cathode was cleaned with the rf off. The laser energy fluence was 0.17 mJ/mm^2 at a $1/e^2$ beam diameter of 0.6 mm. The scan area and the number of shots were 3×3 mm^2 and 7000 shots/mm^2, respectively. During laser cleaning, the base vacuum was varied from 6.0×10^{-7} Pa to 8.0×10^{-7} Pa. The effect of laser cleaning on the *QE* was measured and is discussed below.

3.2 QE of the Mg cathode

The *QE* of the cathode is dependent on the work function of the cathode material and the surface conditions. When an electric field is applied to the cathode, the effective work function of the cathode material is reduced by the Schottky effect. The electron current density can be expressed as

$$J = aI(h\nu - \phi)^2, \tag{1}$$

where

$$\phi = \phi_0 - b\sqrt{\beta E}$$

and

$$b = \sqrt{e/4\pi\varepsilon_0}.$$

I is the laser intensity, $h\nu$ is the incident photon energy, a is a material-dependent constant, ϕ_0 is the work function at zero field, β is the field enhancement factor, E is the applied electric field, e is the electron charge and ε_0 is the dielectric constant. Because *QE* is proportional to J/I, the relationship between *QE* and the effective work function is given by

$$QE \equiv a(h\nu - \phi_0 + b\sqrt{\beta E})^2. \tag{2}$$

This indicates that the *QE* of the photocathode is dependent not only on the incident laser photon energy, but also on the electric field on the surface of the cathode. By rewriting eq. (2), it can be noted that $QE^{0.5}$ versus $E^{0.5}$ is a straight line with a slope of $b^*(a^*\beta)^{0.5}$. The magnitude of the slope is a good indicator of the sensitivity of the cathode to the Schottky effect.

For the measurements of the *QE* of the Mg cathode, the 4th harmonic of the Nd:YLF laser was used. This yielded incident UV laser light at 262 nm (4.74 eV) with a constant peak electric field of 57 MV/m on the surface of the cathode. The spot size of the laser beam on the surface of the cathode had a $1/e^2$ diameter of 3 mm. The laser injection phase of the rf gun was adjusted by using a phase shifter (see Fig. 3) to achieve the maximum bunch charge. Figure 4 shows the bunch charge of the electrons emitted from the Mg cathode as a function of the laser pulse energy before and after the laser cleaning process. A high bunch charge was observed after laser cleaning. The data indicates that the bunch charge of the electrons increased linearly when the incident laser pulse energy was <2 nC for the Mg cathode, while a nonlinearity was observed in the charge increase when the laser pulse energy was >2 nC. This is caused by a space-charge effect close to the cathode surface, i.e., where the beam is not yet relativistic. Fitting the data at <2 nC with eq. (2), the effective *QE* of the Mg cathode was determined to be 8.5×10^{-5} before laser cleaning and 1.0×10^{-3} after laser cleaning.

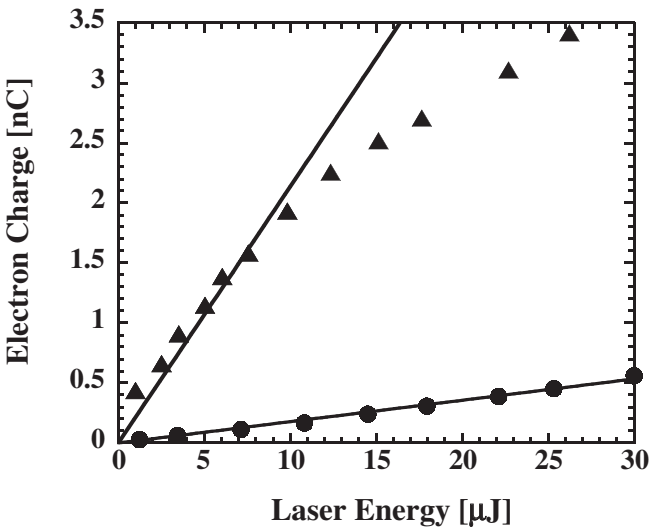

Fig. 4. Emitted electron charge from the Mg cathode as a function of the laser (262 nm) energy before (●) and after (▲) laser cleaning. The lines represent the best fit of the data at <2.0 nC by eq. (2).

We also tried to measure the *QE* of the Mg cathode with 349 nm UV laser light. The 349 nm laser has a photon energy of 3.56 eV, which is lower than the Mg work function. However, according to eq. (1), a photoelectron can be extracted from a cathode under a high electric field via the Schottky effect. Figure 5 shows a plot of the bunch charge of the electrons emitted from the Mg cathode for different laser pulse energies before and after the laser cleaning process. A peak electric field of 57 MV/m on the cathode surface was used in the experiment. The effective *QE* was found to be 1.0×10^{-5} before laser cleaning and 2.2×10^{-5} after laser cleaning. It is noted that, for an incident laser pulse energy of >80 μJ, a harmonic photoemission process takes place; that is, higher energy electrons are emitted from the Mg cathode by absorbing two incident laser photons. However, there may be benefits in using a wavelength of 349 nm for low-charge applications: 1) the light conversion efficiency at 349 nm is larger than that at 262 nm. 2) The effect of the electron thermal normalized emittance could be suppressed.

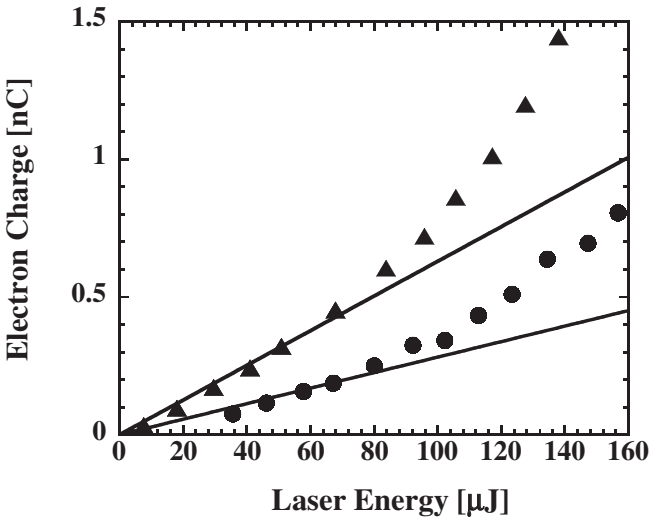

Fig. 5. Emitted electron charge from the Mg cathode as a function of the laser (349 nm) energy before (●) and after (▲) laser cleaning. The lines represent the best fit of the data at the laser energy <80 μJ.

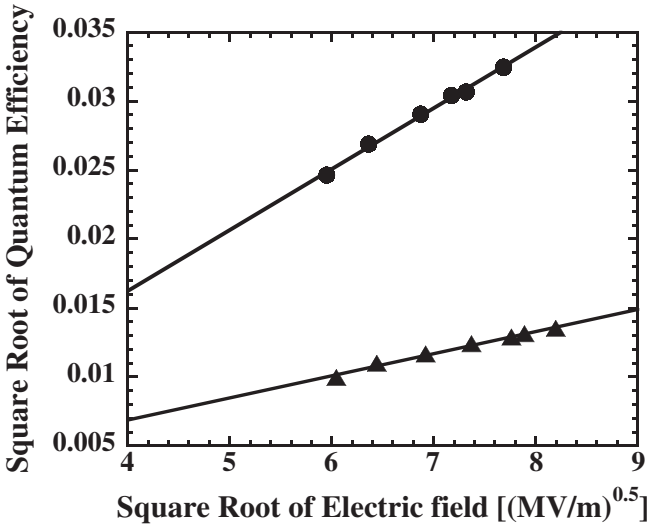

Fig. 6. Results of the *QE* measurement as a function of the peak electric field before (●) and after (▲) laser cleaning. The 262 nm UV laser was used in this experiment.

In order to study the Schottky effect, we changed the input rf power of the rf gun to obtain different peak electric fields on the cathode surface by varying the output of the klystron. The laser injection phase of the rf gun was adjusted for the maximum bunch charge emission at each electric field. Figure 6 shows the results of the *QE* measurement as a function of the peak electric field. The 262 nm UV laser light was used as the incident light in the experiment. In the measurement, the bunch charge was kept at <1 nC for each electric field. This was achieved by adjusting the incident laser pulse energy to avoid charge saturation due to the space-charge effect during the *QE* measurement, as was described above. Good linearity of $QE^{0.5}$ with $E^{0.5}$ was obtained for the Mg cathode before and after laser cleaning. The effect of laser cleaning on the Mg cathode was observed in the measurement.

Table I shows the Mg cathode performance comparing with the BNL's results.[14] The *QE* measurements were carried under a vacuum pressure of 3×10^{-6} Pa which was higher than the operating conditions in the BNL by two orders, resulting in a lower *QE* in the experiment. However, the technique of HIP with diamond polishing is a practical tool for Mg cathode manufacture.

4. Conclusion

A new technique of HIP with diamond polishing was presented for the manufacture of a Mg photocathode. The quantum efficiency of the Mg cathode was measured before and after the laser cleaning process. A high *QE* of up to 1×10^{-3} was achieved under the illumination with 262 nm laser light. The *QE* of the Mg cathode under the illumination with 349 nm laser light was measured to be 2.2×10^{-5}. The dependence of the *QE* on the electric field was measured and compared with the results of a theoretical analysis including

Table I. Summary of the Mg photocathode rf gun.

	SHI	BNL[14]
Manufacture method	Hot isostatic pressing with diamond polishing	Friction welding with diamond polishing
Quantum efficiency at 262 nm laser light	1.0×10^{-3} (after laser cleaning) 8.5×10^{-5} (before laser cleaning)	2×10^{-3} (after laser cleaning) —
Quantum efficiency at 349 nm laser light	2.2×10^{-5} (after laser cleaning) 1.0×10^{-5} (before laser cleaning)	—
Peak rf field	57 MV/m	100–120 MV/m
Rf aging time	3 days	2 days
Dark current	0.2 nC	—
Vacuum pressure in rf gun after rf aging	3×10^{-6} Pa (with rf on)	7×10^{-8} Pa (with rf on)
Surface cleaning	Laser cleaning by 262 nm laser light Cleaning conditions: Fluence: 0.17 mJ/mm^2, Shot no.: 7000 shots/mm^2	Laser cleaning by 262 nm laser light Cleaning conditions: Laser energy: increases till the base pressure rises from 7×10^{-8} Pa to 9×10^{-8} Pa

the Schottky effect under the illumination with 262 nm laser light.

However, there are some remaining studies, such as the *QE* and dark current measurements under a high peak electric field of >100 MV/m. An experiment on multibunch electron beam generation is also planned using the Mg photocathode.

Acknowledgements

This work was performed under the management of a technological research association, the Femtosecond Technology Research Association (FESTA), supported by the New Energy and Industrial Technology Development Organization (NEDO).

1) M. Cornacchia *et al.*: Linac Coherent Light Source (LCLS) Design Study Report, Stanford University-University of California Report No. SLAC-R-521/UC-414, revised 1998.
2) F. Richard *et al.*: TESTA, The Superconducting Electron-Positron Linear Collider with an Integrated X-Ray Laser Laboratory, Technical Design Report, DESY Report No. DESY 2001-011, ISBN 3-935702-00-0, 2001.
3) J. Yang, M. Washio, A. Endo and T. Hori: Nucl. Instrum. Methods Phys. Res. A **428** (1999) 556.
4) M. Yorozu, J. Yang, Y. Okada, T. Yanagida, F. Sakai, K. Takasago, S. Ito and A. Endo: Appl. Phys. B **74** (2002) 327.
5) J. Yang, T. Yanagida, M. Yorozu, F. Sakai, Y. Okada and A. Endo: Rev. Sci. Instrum. **37** (2002) 1752.
6) D. T. Palmer, X. J. Wang, R. H. Miller, M. Babzien, I. Ben-Zvi, C. Pellegrini, J. Sheehan, J. Skaritka, H. Winick, M. Woodle and V. Yakimenko: Proc. Particle Accelerator Conf., Canada, 1998, p. 2687.
7) X. J. Wang and I. Ben-Zvi: Proc. Particle Accelerator Conf., Canada, 1998, p. 2793.
8) J. Yang, F. Sakai, Y. Okada, M. Yorozu, T. Yanagida and A. Endo: Nucl. Instrum. Methods Phys. Res. A **491** (2002) 15.
9) J. Yang, F. Sakai, T. Yanagida, M. Yorozu, Y. Okada, K. Takasago, A. Endo, A. Yada and M. Washio: J. Appl. Phys. **92** (2002) 1608.
10) Y. Aoki, J. Yang, M. Hirose, F. Sakai, A. Tsunemi, M. Yorozu, Y. Okada, A. Endo, X. J. Wang and I. Ben-Zvi: Nucl. Instrum. Methods Phys. Res. A **455** (2000) 99.
11) Y. Suzuki, T. Kozeki, S. Ono, H. Murakami, H. Ohtake, N. Sarukura, T. Nakajyo, F. Sakai and Y. Aoki: Appl. Phys. Lett. **80** (2002) 3280.
12) D. H. Dowell: Proc. SPIE **3614** (1999) 14.
13) T. Srinivasan Rao, I. Ben-Zvi, J. Smedley, X. J. Wang, M. Woodle, D. T. Palmer and R. H. Miller: Proc. Particle Accelerator Conf., Canada, 1998, p. 2790.
14) X. J. Wang, M. Babzien, X. Y. Chang, D. Lynch, S. Pjerov, M. Woodle and Z. Wu: Proc. European Particle Accelerator Conf., France, 2002, p. 1822.